

An NEP_v Approach for Feature Selection via Orthogonal OCCA with the $(2, 1)$ -norm Regularization

Li Wang*

Lei-Hong Zhang[†]Ren-Cang Li[‡]

February 22, 2025

Abstract

A novel feature selection model via orthogonal canonical correlation analysis with the $(2, 1)$ -norm regularization is proposed, and the model is solved by a practical NEP_v approach (nonlinear eigenvalue problem with eigenvector dependency), yielding a feature selection method named OCCA-FS. It is proved that OCCA-FS always produces a sequence of approximations with monotonic objective values and is globally convergent. Extensive numerical experiments are performed to compare OCCA-FS against existing feature selection methods. The numerical results demonstrate that OCCA-FS produces superior classification performance and often comes out on the top among all feature selection methods in comparison.

Keywords: Feature selection, Orthogonal CCA, $(2, 1)$ -norm regularization, Sparse projection, NEP_v

Mathematics Subject Classification 58C40; 65F30; 65H17; 65K05; 90C26

1 Introduction

High-dimensional datasets have been increasingly available due to the rapid development of information technology. Feature selection is one of the most important tools in machine learning. It aims to select a subset of most important features from a large number of original features for a compact and informative representation [6]. As a result, feature selection is generally used as a preprocessing step to remove irrelevant or noisy features and, at the same time, select the most important features, from real-world data before conducting other machine learning tasks, such as classification.

*Department of Mathematics, University of Texas at Arlington, Arlington, TX 76019-0408, USA. Supported in part by NSF DMS-2407692. Email: li.wang@uta.edu.

[†]School of Mathematical Sciences, Soochow University, Suzhou 215006, Jiangsu, China. Supported in part by the National Natural Science Foundation of China (NSFC-12471356, NSFC-12371380), Jiangsu Shuangchuang Project (JSSCTD202209), Academic Degree and Postgraduate Education Reform Project of Jiangsu Province, and China Association of Higher Education under grant 23SX0403. Email: longzlh@suda.edu.cn.

[‡]Department of Mathematics, University of Texas at Arlington, Arlington, TX 76019-0408, USA. Supported in part by NSF DMS-2407692. Email: rccli@uta.edu.

Supervised feature selection (SFS) is a type of a feature selection paradigm where the classification label information is available to guide selection. Methods for SFS generally fall into three categories: filter, wrapper, and embedded [21]. Filter methods, such as T-test [17], rank input features by their intrinsic and statistical characteristics, independent of learning algorithms; Wrapper methods first propose feature subsets and then evaluate them according to certain learning objective, such as SVM in [7]; Embedded methods aim to search for an optimal subset of features by solving some specific mathematical learning model, such as correntropy induced robust feature selection (CRFS) [8].

Least square regression (LSR) is the most common embedded statistical methodology for supervised feature selection. Within the umbrella, there are variations designed for various purposes. In particular, LSR confined to the Stiefel manifold can retain more statistical and structural information [29, 25] than otherwise. For classification, orthogonal least squares regression (OLSR) can preserve more discriminative properties in the projection subspace than the standard LSR and can avoid trivial solutions [3].

Let $X \in \mathbb{R}^{n \times p}$ be an input data matrix whose columns are p sample data points and let $\mathbf{y} \in \{1, \dots, k\}^p$ be the associated class labels, where n is the number of input features, k is the number of class labels. OLSR aims to estimate a linear function

$$f(\mathbf{x}) = P^T \mathbf{x} + \mathbf{b}$$

by minimizing the least square error on the given sample data with respect to the one-hot representation of the class labels \mathbf{y} , where $P \in \mathbb{R}^{n \times k}$ is the linear coefficient matrix restricted to the Stiefel manifold, and $\mathbf{b} \in \mathbb{R}^k$ is the intercept term. Specifically, OLSR determines the linear function $f(\cdot)$ and the intercept term \mathbf{b} by the following optimization problem

$$\min_{P \in \mathbb{O}^{n \times k}, \mathbf{b} \in \mathbb{R}^k} \|(P^T X + \mathbf{b} \mathbf{1}_p^T) - Y\|_{\mathbb{F}}^2, \quad (1.1)$$

where $Y \in \{0, 1\}^{k \times p}$ is the one-hot representation matrix of class labels \mathbf{y} of sample data points, $\mathbf{1}_p \in \mathbb{R}^p$ is the vector of all ones, and

$$\mathbb{O}^{n \times k} = \{P \in \mathbb{R}^{n \times k} : P^T P = I_k\} \subset \mathbb{R}^{n \times k}$$

is the Stiefel manifold. As is commonly done, the intercept term \mathbf{b} can be eliminated by first minimizing the objective of (1.1) over \mathbf{b} , given P , to get $\mathbf{b} = (P^T X - Y) \cdot (1/p) \mathbf{1}_p$. Hence OLSR (1.1) is reduced to

$$\min_{P \in \mathbb{O}^{n \times k}} \|P^T X C_p - Y C_p\|_{\mathbb{F}}^2, \quad (1.2)$$

which will still be referred to as OLSR henceforth, where $C_p = I_p - \frac{1}{p} \mathbf{1}_p \mathbf{1}_p^T \in \mathbb{R}^{p \times p}$ is the centering matrix. OLSR (1.2) is also known as an *unbalanced orthogonal Procrustes problem*, and difficult to solve [5]. Expand the objective of OLSR (1.2) in terms of matrix traces to get

$$\|P^T X C_p - Y C_p\|_{\mathbb{F}}^2 = \text{tr}(P^T A P) - 2 \text{tr}(P^T D) + \text{tr}(Y C_p Y^T),$$

where

$$A = XC_pX^T, \quad D = XC_pY^T. \quad (1.3)$$

Since $\text{tr}(YC_pY^T)$ is a constant, i.e., independent of P , OLSR (1.2) is thus equivalent to

$$\min_{P \in \mathbb{O}^{n \times k}} [\text{tr}(P^TAP) - 2\text{tr}(P^TD)]. \quad (1.4)$$

The mathematical idea behind OLSR (1.4) is to bring P^TXC_p towards YC_p as close as possible in the metric of the matrix Frobenius norm. An alternative idea for the same purpose is via maximizing some kind of ‘‘correlation’’ between P^TXC_p and YC_p . Borrowing the idea from canonical correlation analysis (CCA) in statistics while taking YC_p in its entirety, i.e., without being projected, we naturally define the ‘‘correlation’’ as $\text{tr}^2([P^TXC_p][YC_p]^T) / \text{tr}([P^TXC_p][P^TXC_p]^T)$, leading to the following orthogonal-type CCA formulation, instead of OLSR (1.4),

$$\max_{P \in \mathbb{O}^{n \times k}} \frac{\text{tr}^2(P^TD)}{\text{tr}(P^TAP)}, \quad (1.5)$$

where A and D are as defined in (1.3). Optimization problem in this form appeared previously in [28] and was called the OCCA (orthogonal CCA) subproblem. Henceforth for convenience, it will be abusively referred to as OCCA for short.

For feature selection, the $(2, 1)$ -norm regularization is often employed to induce row sparsity in the linear coefficient matrix P in order to rank features [8, 29]. OCCA (1.5) with the $(2, 1)$ -norm regularization takes the form

$$\max_{P \in \mathbb{O}^{n \times k}} \left\{ f(P) := \frac{[\text{tr}(P^TD)]^2}{\text{tr}(P^TAP)} - \alpha \|P\|_{2,1} \right\}, \quad (1.6)$$

which will be referred to as OCCA21 henceforth, where $\alpha > 0$ is the regularization parameter, and the $(2, 1)$ -norm $\|P\|_{2,1}$ is defined as

$$\|P\|_{2,1} = \sum_{i=1}^n \|P_{(i,:)}\|_2$$

with $\|P_{(i,:)}\|_2$ denoting the vector 2-norm of the i th row vector of P . With a properly chosen regularization parameter α , it is expected that the optimizer of OCCA21 (1.6) have (many) negligible rows, i.e., rows such that $\|P_{(i,:)}\|_2 \ll 1$. Features corresponding to those negligible rows in the sample data points are then considered not important and thus can be deselected, while the rest of the features are selected. In practice, however, this is often performed by sorting all row norms $\|P_{(i,:)}\|_2$ decreasingly and then selecting those features corresponding to first many largest row norms.

The rest of this paper is organized as follows. In section 2, we explore a connection between OCCA21 (1.6) and a recent OLSR-OS (OLS with optimal scaling) model of [29] so as to explain that (1.6) implicitly conceals the optimal scaling in OLSR-OS. In section 3, we establish our NEPv theory on OCCA21 (1.6) and our practical NEPv approach for

numerically solving (1.6), yielding our own feature selection method which we will call OCCA-FS. Extensive numerical experiments on OCCA-FS in comparison with three other the-state-of-art methods are conducted in section 4. Finally conclusions are drawn in section 5.

Notation. $\mathbb{R}^{m \times n}$ is the set of $m \times n$ real matrices, $\mathbb{R}^n = \mathbb{R}^{n \times 1}$, and $\mathbb{R} = \mathbb{R}^1$; $\mathbb{R}_+ := \{x \in \mathbb{R} : x \geq 0\}$ and $\mathbb{R}_{++} := \{x \in \mathbb{R}_+ : x > 0\}$. $I_n \in \mathbb{R}^{n \times n}$ is the identity matrix or simply I if its size is clear from the context, and \mathbf{e}_j is the j th column of I of an apt size.

For $B \in \mathbb{R}^{m \times n}$, B^T stands for the transpose of a matrix/vector B ; $\text{rank}(B)$ is the rank of B , and $B_{(i,:)}$ is the i th row of B . For $A \in \mathbb{R}^{n \times n}$, $A \succ 0$ ($\succeq 0$) means that it is symmetric and positive definite (semi-definite), and accordingly $A \prec 0$ ($\preceq 0$) if $-A \succ 0$ ($\succeq 0$).

The *thin* SVD of $B \in \mathbb{R}^{m \times n}$ ($m \geq n$) refers to $B = U\Sigma V^T$ with

$$\Sigma = \text{diag}(\sigma_1(B), \sigma_2(B), \dots, \sigma_n(B)) \in \mathbb{R}^{n \times n}, U \in \mathbb{O}^{m \times n}, V \in \mathbb{O}^{n \times n}.$$

The singular values $\sigma_j(B)$ are always arranged decreasingly as $\sigma_1(B) \geq \dots \geq \sigma_n(B) \geq 0$. Accordingly, $\|B\|_2$, $\|B\|_F$, and $\|B\|_{\text{tr}}$ are the spectral, Frobenius, and trace norms of B :

$$\|B\|_2 = \sigma_1(B), \quad \|B\|_F = \left(\sum_{i=1}^n [\sigma_i(B)]^2 \right)^{1/2}, \quad \|B\|_{\text{tr}} = \sum_{i=1}^n \sigma_i(B),$$

respectively. The trace norm is also known as the *nuclear norm*. Unless otherwise explicitly stated, SVD always refers to *thin* SVD. With the SVD, a polar decomposition of B is given by $B = QH$ [9] where $Q = UV^T$ and $H = V^T \Sigma V$, and Q is called an *orthogonal polar factor* and it is unique if $\text{rank}(B) = n$ [12, 13].

2 OCCA vs. OLSR

2.1 Connection to OLSR-OS

Recently, the authors in [29] noticed that there could be a mismatch in magnitude between sample data in X and labels in Y which is usually of $O(1)$. Confined to the Stiefel manifold, P cannot compensate large discrepancy in magnitude, if any, between the two. To overcome such a potential discrepancy, they introduced a scaling parameter to better align the magnitudes of sample data points with their labels and called the new model OLSR-OS. Specifically, OLSR-OS determines the linear function $f(\mathbf{x}) = P^T \mathbf{x} + \mathbf{b}$ by

$$\min_{\gamma \in \mathbb{R}, P \in \mathbb{O}^{n \times k}, \mathbf{b} \in \mathbb{R}^k} \|\gamma(P^T X + \mathbf{b}\mathbf{1}_p^T) - Y\|_F^2, \quad (2.1)$$

where γ is a scaling parameter. Similarly, the intercept term \mathbf{b} can be optimized out first to yield

$$\min_{\gamma \in \mathbb{R}, P \in \mathbb{O}^{n \times k}} \|P^T(\gamma X)C_p - YC_p\|_F^2. \quad (2.2)$$

Expand the objective of OLSR-OS (2.2) in terms of matrix traces to get

$$\|P^T(\gamma X)C_p - YC_p\|_F^2 = \gamma^2 \text{tr}(P^T A P) - 2\gamma \text{tr}(P^T D) + \text{tr}(YC_p Y^T),$$

where A and D are as in (1.3). Hence OLSR-OS (2.2) is equivalent to

$$\min_{P \in \mathbb{O}^{n \times k}, \gamma \in \mathbb{R}} \left\{ g(P, \gamma) := \gamma^2 \operatorname{tr}(P^T A P) - 2\gamma \operatorname{tr}(P^T D) \right\}. \quad (2.3)$$

Evidently $A \succeq 0$ in (1.3), but we will further assume $\operatorname{rank}(A) > n - k$, which is needed to ensure $\operatorname{tr}(P^T A P) > 0$ for any $P \in \mathbb{O}^{n \times k}$ and hence $g(P, \gamma)$ is always bounded from below for $\gamma \in \mathbb{R}$. Given P , $g(P, \gamma)$ over $\gamma \in \mathbb{R}$ achieves its minimum at

$$\gamma = \frac{\operatorname{tr}(P^T D)}{\operatorname{tr}(P^T A P)}, \quad (2.4)$$

substituting which into (2.3), upon considering maximizing $-g(P, \gamma)$ instead, turns (2.3) equivalently into OCCA (1.5). In other words, OCCA (1.5) is OLSR-OS (2.3) with scaling parameter γ optimized out.

It is noted that any discrepancy in magnitude between X and Y does not influence the optimizers to OCCA (1.5) at all, which is not surprising because the above connection simply implies there is some optimal scaling inherently.

Upon introducing the $(2, 1)$ -norm regularization, we end up with OCCA21 (1.6), the model of OCCA regularized by the $(2, 1)$ -norm. In section 3, we will focus on the NEPv theory for OCCA21 (1.6) and how to numerically solve it by a practical NEPv approach.

2.2 Solving regularized OLSR-OS

In [29], the authors combined OLSR-OS (2.3) with the $(2, 1)$ -norm regularization

$$\min_{P \in \mathbb{O}^{n \times k}, \gamma \in \mathbb{R}} \left\{ g(P, \gamma) := \gamma^2 \operatorname{tr}(P^T A P) - 2\gamma \operatorname{tr}(P^T D) + \alpha \|P\|_{2,1} \right\}, \quad (2.5)$$

which will be referred to as OLSR-OS21 henceforth. Also in [29], an alternating optimization procedure between γ and P was designed to solve (2.5), yielding an eventual supervised feature selection method named PEB-FS.

Unfortunately, the alternating optimization procedure is not properly done. We shall now explain. PEB-FS [29] solves (2.5) alternatingly between γ and P with

the γ -update: minimize $g(P, \gamma)$ over γ given P , and
the P -update: minimize $g(P, \gamma)$ over P given γ .

The γ -update is rather easy and has a close-form solution in (2.4), but the P -update is not and that is where the mistake was committed. Specifically, to find the P -update, in [29], the authors rewrite $g(P, \gamma)$ as follows. Let

$$\Gamma(P) = \operatorname{diag}(\|P_{(1,:)}\|_2^{-1}, \|P_{(2,:)}\|_2^{-1}, \dots, \|P_{(n,:)}\|_2^{-1}), \quad (2.6a)$$

and let $P_\perp \in \mathbb{O}^{n \times (n-k)}$ such that $Q := [P, P_\perp] \in \mathbb{O}^{n \times n}$. Then we have

$$\|P\|_{2,1} = \operatorname{tr}(\Gamma(P) P P^T) = \operatorname{tr}(P^T \Gamma(P) P), \quad (2.6b)$$

$$g(P, \gamma) = \text{tr}(Q^T[\gamma^2 A + \alpha\Gamma(P)]Q) - 2\gamma \text{tr}(Q^T R(P)), \quad (2.6c)$$

where $R(P) := [D, (\gamma/2)AP_\perp + (\alpha/(2\gamma))\Gamma(P)P_\perp] \in \mathbb{R}^{n \times n}$. Now given γ , if $\Gamma(P)$ were constant (i.e., independent of P), then $\text{tr}(Q^T[\gamma^2 A + \alpha\Gamma(P)]Q)$ would be constant too, and thus minimizing $g(P, \gamma)$ over P would be equivalent to maximizing $\text{tr}(Q^T R(P))$, which could be done by the SVD of $R(P)$ if $R(P)$ were also constant. Unfortunately, both $\Gamma(P)$ and $R(P)$ are in general dependent of P , and hence minimizing $g(P, \gamma)$ over P , given γ , cannot be simply done by the SVD of $R(P)$ evaluated at the current approximation, but that is exactly what the P -update was carried out in [29]. For that reason, the conclusion of [29, Theorem 3.2] that PEB-FS generates monotonically decreasing objective values is not correct. In fact, later in Figure 4.1 it is observed that objective values by PEB-FS is not monotonically decreasing on dataset Yale. Also in the figure, we see that the optimal objective values by OCCA-FS is far smaller than those delivered by PEB-FS for all considered datasets.

It is noted that the P -update can be handled by the NEPv approach in a similar way to what we will do to OCCA21 (1.6) in the next section. For that, we will simply make a remark later in Remark 3.2 but will not pursue it in this paper because OCCA21 (1.6) can merge both updates into one, kind of “kill two birds with one stone!”

3 NEPv for OCCA with the (2,1)-norm regularization

Earlier, we mentioned that the role of α in OCCA21 (1.6), and in OLSR-OS21 (2.5) for that matter, is to drive some rows of the respective optimizers towards 0. But owing to the fact that $P \in \mathbb{O}^{n \times k}$, P has at least k rows that have nontrivial norms, i.e., not small, as guaranteed by Theorem 3.1 below.

Theorem 3.1. *Let $P \in \mathbb{O}^{n \times k}$ and rearrange $\{\|P_{(i,:)}\|_2\}_{i=1}^n$ descendingly as*

$$\|P_{(i_1,:)}\|_2 \geq \|P_{(i_2,:)}\|_2 \geq \cdots \geq \|P_{(i_n,:)}\|_2.$$

Then

$$\|P_{(i_j,:)}\|_2 \geq \sqrt{\frac{k-j+1}{n-j+1}} \geq \frac{1}{\sqrt{n-k+1}} \quad \text{for } 1 \leq j \leq k.$$

Proof. For $1 \leq j \leq k$, noticing $\|P_{(i,:)}\|_2 \leq 1$ for any i , we have

$$k = \sum_{j=1}^n \|P_{(i_j,:)}\|_2^2 \leq (j-1) + (n-j+1)\|P_{(i_j,:)}\|_2^2,$$

implying

$$\|P_{(i_j,:)}\|_2^2 \geq \frac{k-j+1}{n-j+1} \geq \frac{1}{n-k+1},$$

as was to be shown. □

3.1 The NEPv Approach

We rewrite $\|P\|_{2,1}$ in terms of matrix traces as follows:

$$\|P\|_{2,1} = \sum_{i=1}^n \|\mathbf{e}_i^T P\|_2 = \sum_{i=1}^n \sqrt{\mathbf{e}_i^T P P^T \mathbf{e}_i} = \sum_{i=1}^n \sqrt{\text{tr}(P^T \mathbf{e}_i \mathbf{e}_i^T P)}, \quad (3.1)$$

and, hence, for OCCA21 (1.6),

$$f(P) = \frac{[\text{tr}(P^T D)]^2}{\text{tr}(P^T A P)} - \alpha \sum_{i=1}^n \sqrt{\text{tr}(P^T \mathbf{e}_i \mathbf{e}_i^T P)} \quad (3.2a)$$

$$= \phi \circ T(P), \quad (3.2b)$$

where, for $\mathbf{x} \equiv [x_i] \in \mathbb{R}^{n+2}$,

$$\phi(\mathbf{x}) = \frac{x_2^2}{x_1} - \alpha \sum_{i=1}^n \sqrt{x_{i+2}}, \quad T(P) = \begin{bmatrix} \text{tr}(P^T A P) \\ \text{tr}(P^T D) \\ \text{tr}(P^T \mathbf{e}_1 \mathbf{e}_1^T P) \\ \vdots \\ \text{tr}(P^T \mathbf{e}_n \mathbf{e}_n^T P) \end{bmatrix}. \quad (3.2c)$$

Function $\phi(\mathbf{x})$ is convex in its first two components in $\mathbb{R}_{++} \times \mathbb{R}$ [2, p.72] and componentwise convex in the rest of its components in \mathbb{R}_+ because

$$\frac{d^2(-\alpha\sqrt{x})}{dx^2} = \frac{1}{4}\alpha x^{-3/2} \geq 0.$$

Hence $\phi(\mathbf{x})$ is convex for $\mathbf{x} \in \mathbb{R}_{++} \times \mathbb{R} \times \mathbb{R}_+^n$. In other words, $f(P)$ is a convex composition of $n+2$ matrix trace functions: $\text{tr}(P^T A P)$, $\text{tr}(P^T D)$, $\text{tr}(P^T \mathbf{e}_i \mathbf{e}_i^T P)$ for $1 \leq i \leq n$, all of which are atomic functions for NEPv [15, Theorems 7.4 and 7.5]. Therefore it is natural to ask if the NEPv approach [15, Part II] can be utilized to solve (1.6).

In what follows, we will present the NEPv approach for the current case. Let

$$h(P) = \frac{\text{tr}(P^T D)}{\text{tr}(P^T A P)}. \quad (3.3)$$

We have

$$\mathcal{H}(P) := \frac{\partial f(P)}{\partial P} = 2h(P)[D - h(P)AP] - \alpha \sum_{i=1}^n \frac{\mathbf{e}_i \mathbf{e}_i^T P}{\sqrt{\text{tr}(P^T \mathbf{e}_i \mathbf{e}_i^T P)}}, \quad (3.4a)$$

unless some $\text{tr}(P^T \mathbf{e}_i \mathbf{e}_i^T P) = \|\mathbf{e}_i^T P\|_2^2 = 0$ for which case $f(P)$ is not differentiable. As a result, the first order optimality condition, also known as the KKT condition, is [15, section 2]

$$\mathcal{H}(P) = P\Lambda, \quad P \in \mathbb{O}^{n \times k}, \quad \Lambda = \Lambda^T \in \mathbb{R}^{k \times k}, \quad (3.4b)$$

which governs any KKT point P that has no zero rows.

To apply the NEPv approach, we will need a symmetric matrix-valued function that can be constructed from each individual ones for the $n+2$ matrix trace functions: $\text{tr}(P^T A P)$, $\text{tr}(P^T D)$, $\text{tr}(P^T \mathbf{e}_i \mathbf{e}_i^T P)$ for $1 \leq i \leq n$, as atomic functions for NEPv. According to [15, (8.3)], we can use

$$H(P) := 2h(P)[(DP^T + PD^T) - h(P)A] - \alpha \sum_{i=1}^n \frac{\mathbf{e}_i \mathbf{e}_i^T}{\sqrt{\text{tr}(P^T \mathbf{e}_i \mathbf{e}_i^T P)}} \in \mathbb{R}^{n \times n}, \quad (3.5a)$$

whose associated NEPv is

$$H(P)P = P\Omega, \quad P \in \mathbb{O}^{n \times k}, \quad \Omega = \Omega^T \in \mathbb{R}^{k \times k}. \quad (3.5b)$$

We find that for $P \in \mathbb{O}^{n \times k}$

$$H(P)P - \mathcal{H}(P) = P[2h(P)D^T P]. \quad (3.6)$$

The next theorem is a straightforward consequence of [15, Theorem 6.1] and (3.6).

Theorem 3.2 ([15, Theorem 6.1]). *Suppose that (2.5) has no KKT point P with zero rows. $P \in \mathbb{O}^{n \times k}$ is a solution to the KKT condition (3.4) if and only if it is a solution to NEPv (3.5) and $D^T P$ is symmetric.*

We restate [15, Theorem 8.1] for the current case as follows.

Theorem 3.3 ([15, Theorem 8.1]). *Consider (1.6) with $f(P)$ as in (3.2). Let $H(P)$ be given by (3.5a) and*

$$\mathbb{P} := \{P \in \mathbb{O}^{n \times k} : P^T D \succeq 0\} \subseteq \mathbb{O}^{n \times k}. \quad (3.7)$$

For $\hat{P} \in \mathbb{O}^{n \times k}$ and $P \in \mathbb{P}$, if P has no zero rows and if

$$\text{tr}(\hat{P}^T H(P) \hat{P}) \geq \text{tr}(P^T H(P) P) + \eta \quad \text{for some } \eta \in \mathbb{R}, \quad (3.8)$$

then $f(\tilde{P}) \geq f(P) + \eta/2$, where $\tilde{P} = \hat{P}Q \in \mathbb{P}$ with Q being an orthogonal polar factor of $\hat{P}^T D$.

We have stated a seemingly beautiful theory, but there is one unsettling condition in both Theorems 3.2 and 3.3: P has no zero rows. The condition has to be there because of the singularity in the expression of $\mathcal{H}(P)$ in (3.4a) and that of $H(P)$ in (3.5) when one or more rows of P are 0. In order not to miss out any KKT points, we will have to look for those KKT points with one or more zero rows. This can be done, in theory, by exhausting all possibilities, e.g., looking for KKT points P with zero rows. The number of all possibilities is 2^{n-k} because of Theorem 3.1, making this option theoretically correct but practically infeasible.

3.2 A practical NEPv approach

The precise purpose of introducing the (2,1)-norm regularization in (1.6) and (2.5) is to promote row sparsity in P , i.e., making some of the rows of P zeros in theory. When that happens, singularities occur, as they are exposed in (3.4a) and (3.5a). Numerically, it is unlikely that some rows of P become zeros exactly during any optimization process, but near singularity is bound to occur and near-singularity can cause numerical ill-behavior. Fortunately, near-singularity can be effectively monitored by checking if some $\|\mathbf{e}_i^T P\|_2 \ll 1$. When $\|\mathbf{e}_i^T P\|_2 \ll 1$, it means that, from the feature selection point of view, the i th feature is insignificant and may be deselected. In practice, this can be realized by pre-selecting a small tolerance ε_0 and then regarding any rows such that $\|\mathbf{e}_i^T P\|_2 \leq \varepsilon_0$ insignificant. How small should ε_0 be? Since

$$\sum_{i=1}^n \|\mathbf{e}_i^T P\|_2^2 = k \quad \Rightarrow \quad \frac{k}{n} \leq \max_{1 \leq i \leq n} \|\mathbf{e}_i^T P\|_2^2 \leq 1.$$

For data science applications, $\varepsilon_0 = 10^{-3} \sqrt{k/n}$ should be good enough.

In view of these discussions, instead of (1.6), we may solve a perturbed problem of it:

$$\max_{P \in \mathbb{O}^{n \times k}} \left\{ f_{\varepsilon_0}(P) := \frac{[\text{tr}(P^T D)]^2}{\text{tr}(P^T A P)} - \alpha \sum_{i=1}^n \sqrt{\text{tr}(P^T \mathbf{e}_i \mathbf{e}_i^T P) + \varepsilon_0^2} \right\}. \quad (3.9)$$

With the same $T(P)$ as in (3.2c), we find that

$$f_{\varepsilon_0}(P) = \phi_{\varepsilon_0} \circ T(P) \quad \text{with} \quad \phi_{\varepsilon_0}(\mathbf{x}) = \frac{x_2^2}{x_1} - \alpha \sum_{i=1}^n \sqrt{x_{i+2} + \varepsilon_0^2},$$

Function $\phi_{\varepsilon_0}(\mathbf{x})$ is still convex for $\mathbf{x} \in \mathbb{R}_{++} \times \mathbb{R} \times \mathbb{R}_+^n$. Accordingly, we have

$$\mathcal{H}_{\varepsilon_0}(P) := \frac{\partial f_{\varepsilon_0}(P)}{\partial P} = 2h(P)[D - h(P)AP] - \alpha \sum_{i=1}^n \frac{\mathbf{e}_i \mathbf{e}_i^T P}{\sqrt{\text{tr}(P^T \mathbf{e}_i \mathbf{e}_i^T P) + \varepsilon_0^2}}, \quad (3.10a)$$

where $h(P)$ is as defined in (3.3), and the first order optimality condition of (3.9) is then given by [15, section 2]

$$\mathcal{H}_{\varepsilon_0}(P) = PA, \quad P \in \mathbb{O}^{n \times k}, \quad A = A^T \in \mathbb{R}^{k \times k}. \quad (3.10b)$$

Correspondingly, we use symmetric matrix-valued function

$$H_{\varepsilon_0}(P) := 2h(P)[(DP^T + PD^T) - h(P)A] - \alpha \sum_{i=1}^n \frac{\mathbf{e}_i \mathbf{e}_i^T}{\sqrt{\text{tr}(P^T \mathbf{e}_i \mathbf{e}_i^T P) + \varepsilon_0^2}} \in \mathbb{R}^{n \times n}, \quad (3.11a)$$

whose associated NEPv is

$$H_{\varepsilon_0}(P)P = P\Omega, \quad P \in \mathbb{O}^{n \times k}, \quad \Omega = \Omega^T \in \mathbb{R}^{k \times k}. \quad (3.11b)$$

Algorithm 3.1 The NEPv approach for solving (3.9)

Input: $0 \preceq A \in \mathbb{R}^{n \times n}$ (such that $\text{rank}(A) > n - k$), $D \in \mathbb{R}^{n \times k}$, regularization parameter $\alpha > 0$, $\varepsilon_0 > 0$, $H_{\varepsilon_0}(\cdot)$ as (3.11a), and initial $P^{(0)} \in \mathbb{O}^{n \times k}$;

Output: an approximate maximizer of (3.9).

- 1: if $[P^{(0)}]^T D \not\preceq 0$, update $P^{(0)}$ to $P^{(0)}Q_0$ where $Q_0 = U_0V_0^T$, an orthogonal polar factor of $[P^{(0)}]^T D = U_0\Sigma_0V_0$ (SVD);
 - 2: **for** $j = 0, 1, \dots$ until convergence **do**
 - 3: compute $H_j = H_{\varepsilon_0}(P^{(j)}) \in \mathbb{R}^{n \times n}$;
 - 4: solve symmetric eigenvalue problem $H_j\hat{P}^{(j)} = \hat{P}^{(j)}\Omega_j$ for $\hat{P}^{(j)} \in \mathbb{R}^{n \times k}$, an orthonormal basis matrix of the eigenspace associated with the first k largest eigenvalues of H_j ;
 - 5: compute the SVD $[\hat{P}^{(j)}]^T D = U_j\Sigma_jV_j$ and let $Q_j = U_jV_j^T$, an orthogonal polar factor of $[\hat{P}^{(j)}]^T D$;
 - 6: let $P^{(j+1)} = \hat{P}^{(j)}Q_j$;
 - 7: **end for**
 - 8: **return** the last $P^{(j)}$.
-

Again we find that for $P \in \mathbb{O}^{n \times k}$

$$H_{\varepsilon_0}(P)P - \mathcal{H}_{\varepsilon_0}(P) = P[2h(P)D^T P]. \quad (3.12)$$

We will also have the corresponding versions of Theorems 3.2 and 3.3 for (3.9), without the need to assume that P has no zero rows. They are stated as follows.

Theorem 3.4 ([15, Theorem 6.1]). $P \in \mathbb{O}^{n \times k}$ is a solution to the KKT condition (3.10) of (3.9) if and only if it is a solution to NEPv (3.11) and $D^T P$ is symmetric.

Theorem 3.5. Let $H_{\varepsilon_0}(P)$ be given by (3.11) and \mathbb{P} as defined in (3.7).

(a) [15, Theorem 8.1] For $\hat{P} \in \mathbb{O}^{n \times k}$ and $P \in \mathbb{P}$, if

$$\text{tr}(\hat{P}^T H_{\varepsilon_0}(P) \hat{P}) \geq \text{tr}(P^T H_{\varepsilon_0}(P) P) + \eta \quad \text{for some } \eta \in \mathbb{R}, \quad (3.13)$$

then $f_{\varepsilon_0}(\hat{P}) \geq f_{\varepsilon_0}(P) + \eta/2$, where $\tilde{P} = \hat{P}Q \in \mathbb{P}$ with Q being an orthogonal polar factor of $\hat{P}^T D$.

(b) Let $P_* \in \mathbb{O}^{n \times k}$ be an maximizer of (3.9). Then $P_* \in \mathbb{P}$, and P_* satisfies NEPv (3.11b), and the eigenvalues of $\Omega_* := P_*^T H_{\varepsilon_0}(P_*) P_*$ are the k largest eigenvalues of $H_{\varepsilon_0}(P_*)$.

Proof. As cited, item (a) is due to [15, Theorem 8.1]. For item (b), if we can show that $P_* \in \mathbb{P}$ then the rest follows from [15, Theorem 6.3]. Assume, to the contrary, that $P_* \notin \mathbb{P}$, i.e., $P_*^T D \not\preceq 0$, which implies [28, Lemma 3] $\text{tr}(P_*^T D) < \|P_*^T D\|_{\text{tr}} = \text{tr}([P_*Q]^T D)$ where Q is an orthogonal polar factor of $P_*^T D$. Hence $f_{\varepsilon_0}(P_*Q) > f_{\varepsilon_0}(P_*)$, a contradiction, and thus $P_* \in \mathbb{P}$. \square

We point out that, in the proof above, updating P_* to P_*Q is rather standard and popularly used lately in [15, 16, 23, 24, 28, 27].

An self-consistent-field (SCF) iteration to solve (3.11b) is outlined in Algorithm 3.1. A few comments regarding its implementation are in order.

(1) A reasonable stopping criterion at Line 2 is

$$\varepsilon_{\text{KKT}}(P) := \frac{\|\mathcal{H}_{\varepsilon_0}(P) - PA_{\varepsilon_0}(P)\|_{\text{F}}}{2h(P)[\|D\|_{\text{F}} + h(P)\|A\|_{\text{F}}] + n\alpha} \leq \epsilon, \quad (3.14)$$

where $A_{\varepsilon_0}(P) := (P^{\text{T}}\mathcal{H}_{\varepsilon_0}(P) + [\mathcal{H}_{\varepsilon_0}(P)]^{\text{T}}P)/2$ and ϵ is a preselected tolerance.

(2) According to Theorem 3.3, there is no need to compute the partial eigendecomposition at Line 4 accurately up to the working precision but rather it suffices to make (3.13) with a relatively large $\eta > 0$. This is helpful for overall computational efficiency when n is large and the partial eigendecomposition is computed iteratively [4, 14, 18, 20].

Finally with Theorem 3.5(a), the general convergence theorems, [15, Theorems 6.3 and 6.4], apply. To save space, we omit stating them here.

3.3 Acceleration via LOCG

Algorithm 3.1 involves solving a large eigenvalue problem if there are hugely many features in sample data. One option is to employ an iterative eigen-solver. Another option is to borrow the idea of the locally optimal conjugate gradient technique (LOCG), which draws inspiration from optimization [19, 22] and has been increasingly used for linear systems and eigenvalue problems [1, 10, 11, 14, 26] and more recently in [23] for maximizing the sum of coupled traces and in [15] for general optimization on the Stiefel manifold.

Without loss of generality, let $P^{(-1)} \in \mathbb{O}^{n \times k}$ be the approximate maximizer of (3.9) from the very previous iterative step, and $P \in \mathbb{O}^{n \times k}$ the current approximate maximizer. We are now looking for the next approximate maximizer $P^{(1)}$, along the line of LOCG, according to

$$P^{(1)} = \arg \max_{Y \in \mathbb{O}^{n \times k}} f_{\varepsilon_0}(Y), \text{ s.t. } \mathcal{R}(Y) \subseteq \mathcal{R}([P, \mathcal{R}(P), P^{(-1)}]), \quad (3.15)$$

where $\mathcal{R}(\cdot)$ is the column subspace of a matrix, and $\mathcal{R}(P)$ is the gradient of $f_{\varepsilon_0}(\cdot)$ at P with respect to the Stiefel manifold:

$$\mathcal{R}(P) = \mathcal{H}_{\varepsilon_0}(P) - P \cdot \frac{1}{2} \left[P^{\text{T}} \mathcal{H}_{\varepsilon_0}(P) + \mathcal{H}_{\varepsilon_0}(P)^{\text{T}} P \right]. \quad (3.16)$$

Initially for the first iteration, we don't have $P^{(-1)}$ and it is understood that $P^{(-1)}$ is absent from (3.15), i.e., simply $\mathcal{R}(Y) \subseteq \mathcal{R}([P, \mathcal{R}(P)])$.

We still have to numerically solve (3.15). For that purpose, let $W \in \mathbb{O}^{n \times m}$ be an orthonormal basis matrix of subspace $\mathcal{R}([P, \mathcal{R}(P), P^{(-1)}])$. Generically, $m = 3k$ but $m < 3k$ can happen. It can be implemented by the Gram-Schmidt orthogonalization process,

starting with orthogonalizing the columns of $\mathcal{R}(P)$ against P since $P \in \mathbb{O}^{n \times k}$ already. In MATLAB, to fully take advantage of its optimized functions, we simply set $W = [\mathcal{R}(P), P^{(-1)}]$ (or $W = \mathcal{R}(P)$ for the first iteration) and then do

$$\boxed{\begin{array}{l} W=W-P*(P'*W); W=orth(W); W=W-P*(P'*W); W=orth(W); \\ W=[P,W]; \end{array}} \quad (3.17)$$

where the first line performs the classical Gram-Schmidt orthogonalization twice to almost ensure that the resulting columns of W are fully orthogonal to the columns of P at the end of the first line, and `orth` is a MATLAB function for orthogonalization, which uses the thin SVD. Another alternative is the thin QR $[W, \sim]=qr(W, 0)$ and is cheaper than `orth`. It is important to note that the first k columns of the final W are the same as those of P .

Now it follows from $\mathcal{R}(Y) \subseteq \mathcal{R}([P, \mathcal{R}(P), P^{(-1)}]) = \mathcal{R}(W)$ that in (3.15)

$$Y = WZ \quad \text{for } Z \in \mathbb{O}^{m \times k}. \quad (3.18a)$$

Problem (3.15) becomes

$$Z_{\text{opt}} = \arg \max_{Z \in \mathbb{O}^{m \times k}} \tilde{f}_{\varepsilon_0}(Z), \quad (3.18b)$$

where, upon setting $\tilde{A} = W^T A W$, $\tilde{D} = W^T D$, and $\mathbf{w}_i^T = \mathbf{e}_i^T W$,

$$\tilde{f}_{\varepsilon_0}(Z) := f_{\varepsilon_0}(WZ) = \frac{[\text{tr}(Z^T \tilde{D})]^2}{\text{tr}(Z^T \tilde{A} Z)} - \alpha \sum_{i=1}^n \sqrt{\text{tr}(Z^T \mathbf{w}_i \mathbf{w}_i^T Z) + \varepsilon_0^2}. \quad (3.18c)$$

Finally $P^{(1)} = W Z_{\text{opt}}$ for (3.15). Note that $\tilde{f}_{\varepsilon_0}(Z)$ takes the same form as $f_{\varepsilon_0}(P)$ in (3.9) and the theory in the previous subsection for (3.9) can be extended straightforwardly. In particular, the KKT condition is

$$\tilde{\mathcal{H}}_{\varepsilon_0}(Z) = Z \tilde{\Lambda}, \quad Z \in \mathbb{O}^{n \times k}, \quad \tilde{\Lambda} = \tilde{\Lambda}^T \in \mathbb{R}^{k \times k}, \quad (3.19a)$$

where

$$\tilde{\mathcal{H}}_{\varepsilon_0}(Z) := \frac{\partial \tilde{f}(Z)}{\partial Z} = 2\tilde{h}(Z)[\tilde{D} - \tilde{h}(Z) \tilde{A} Z] - \alpha \sum_{i=1}^n \frac{\mathbf{w}_i \mathbf{w}_i^T Z}{\sqrt{\text{tr}(Z^T \mathbf{w}_i \mathbf{w}_i^T Z) + \varepsilon_0^2}}, \quad (3.19b)$$

$\tilde{h}(Z) = \text{tr}(Z^T \tilde{D}) / \text{tr}(Z^T \tilde{A} Z)$, and the associated NEPv is

$$\tilde{H}_{\varepsilon_0}(Z) Z = Z \tilde{\Omega}, \quad Z \in \mathbb{O}^{m \times k}, \quad \tilde{\Omega} = \tilde{\Omega}^T \in \mathbb{R}^{k \times k}, \quad (3.20a)$$

where

$$\tilde{H}_{\varepsilon_0}(Z) := 2\tilde{h}(Z)[(\tilde{D} Z^T + Z \tilde{D}^T) - \tilde{h}(Z) \tilde{A}] - \alpha \sum_{i=1}^n \frac{\mathbf{w}_i \mathbf{w}_i^T}{\sqrt{\text{tr}(Z^T \mathbf{w}_i \mathbf{w}_i^T Z) + \varepsilon_0^2}} \in \mathbb{R}^{m \times m}, \quad (3.20b)$$

a much smaller matrix. There are corresponding versions of both Theorems 3.4 and 3.5 and, in principle, Algorithm 3.1 can be used to solve NEPv (3.20). Algorithm 3.2 outlines an accelerating version of Algorithm 3.1.

Algorithm 3.2 The LOCG-accelerated NEPv approach for solving (3.9)

Input: $0 \preceq A \in \mathbb{R}^{n \times n}$ (such that $\text{rank}(A) > n - k$), $D \in \mathbb{R}^{n \times k}$, regularization parameter $\alpha > 0$, $\varepsilon_0 > 0$, and initial $P^{(0)} \in \mathbb{O}^{n \times k}$;

Output: an approximate maximizer of (3.9).

- 1: if $[P^{(0)}]^T D \not\approx 0$, update $P^{(0)}$ to $P^{(0)}Q_0$ where $Q_0 = U_0V_0^T$, an orthogonal polar factor of $[P^{(0)}]^T D = U_0\Sigma_0V_0$ (SVD);
 - 2: $P^{(-1)} = []$; % null matrix
 - 3: **for** $j = 0, 1, \dots$ until convergence **do**
 - 4: compute $W \in \mathbb{O}^{n \times m}$ such that $\mathcal{R}(W) = \mathcal{R}([P^{(j)}, \mathcal{R}(P^{(j)}), P^{(j-1)}])$ as in (3.17), where $\mathcal{R}(P^{(j)})$ is calculated according to (3.16);
 - 5: solve (3.18b) for Z_{opt} by Algorithm 3.1 with inputs $\tilde{A}, \tilde{D}, \tilde{H}_{\varepsilon_0}(\cdot)$ in (3.20b), initially $Z^{(0)}$ being the first k columns of I_m ;
 - 6: $P^{(j+1)} = WZ_{\text{opt}}$;
 - 7: **end for**
 - 8: **return** the last $P^{(j)}$.
-

Remark 3.1. There are a few comments in order, regarding Algorithm 3.2.

- (i) The stopping criterion (3.14) can be used at Line 3;
- (ii) It is important to compute W at Line 4 in such a way, as explained moments ago in (3.17), that its first k columns are exactly the same as those of $P^{(j)}$. This is because as $P^{(j)}$ converges, $P^{(j+1)}$ changes little from $P^{(j)}$ and hence Z_{opt} is increasingly close to the first k columns of I_m . This explains the choice of $Z^{(0)}$ at Line 5.
- (iii) At Line 5, some saving can be achieved by reusing quantities that are already computed. For example, we may use

$$AP^{(j+1)} = (AW)Z_{\text{opt}}, \quad [P^{(j+1)}]^T AP^{(j+1)} = Z_{\text{opt}}^T (W^T AW)Z_{\text{opt}}$$

to compute the next $AP^{(j+1)}$ and $[P^{(j+1)}]^T AP^{(j+1)}$ at costs $O(nk^2)$ and $O(k^3)$, respectively, instead of $O(n^2k)$ by reusing AW and $W^T AW$.

- (iv) An area of improvement is to solve (3.18b) with an accuracy, comparable but fractionally better than the current $P^{(j)}$ as an approximate solution of (3.9). Specifically, if we use (3.14) at Line 3 here to stop the for-loop: Lines 3–7, with tolerance ϵ , then instead of using the same ϵ for Algorithm 3.1 at its Line 2, we can use a fraction, say $1/8$, of $\varepsilon_{\text{KKT}}(P)$ evaluated at the current approximation $P = P^{(j)}$ as stopping tolerance within Algorithm 3.1.

Remark 3.2. In subsection 2.2, we outlined how OLSR-OS21 (2.5) is alternately solved in [29] and explained a mistake in its P -update calculation, causing inferior performance by PEB-FS in the next section. We point out that the P -update can be handled analogously by the NEPv approach we laid out in this section upon noticing that (2.5) is equivalent to

$$\max_{P \in \mathbb{O}^{n \times k}, \gamma \in \mathbb{R}} \left\{ \tilde{f}(P, \gamma) := -\gamma^2 \text{tr}(P^T AP) + 2\gamma \text{tr}(P^T D) - \alpha \|P\|_{2,1} \right\}, \quad (3.21)$$

and, with the same $T(\cdot)$ as in (3.2c), $\tilde{f}(P, \gamma) = \tilde{\phi} \circ T(P)$, where

$$\tilde{\phi}(\mathbf{x}; \gamma) = -\gamma^2 x_1 + 2\gamma x_2 - \alpha \sum_{i=1}^n \sqrt{x_{i+2}} \quad \text{for } \mathbf{x} = [x_i] \in \mathbb{R}^{n+2}.$$

It can be seen that, given γ , $\tilde{\phi}(\mathbf{x}; \gamma)$ is convex for $\mathbf{x} \in \mathbb{R}^2 \times \mathbb{R}_+^n$.

4 Numerical Experiments

As we commented earlier, the role of the $(2, 1)$ -norm regularization is to induce row sparsity in an optimizer P to the optimization problem (1.6) or (2.5). In practice, often, as we do in section 3, $\|P\|_{2,1}$ is perturbed slightly to avoid singularity numerically. It is done by regularizing the 2-norms of the rows of P as in subsection 3.2, where it is suggested to use $\varepsilon_0 = 10^{-3} \sqrt{k/n}$. At the end of computations, an approximate optimizer P is obtained, and any rows of P such that $\|\mathbf{e}_i^T P\|_2 \leq \varepsilon_0$ is regarded as 0 numerically for the purpose of feature selection. Practically, the norms of the rows of P are calculated and sorted descendingly, and we then select the q features corresponding to the q largest row norms of P , where q is pre-chosen. Theoretically, it only makes sense to use $q \geq k$ due to Theorem 3.1, and yet practitioners may still select fewer than k features regardless, as in [29]. We shall follow this practice in our experiments, too.

4.1 Experimental setting

Six benchmark datasets are used in our experiments to demonstrate the effectiveness of the proposed feature selection method. They are COIL20¹, COIL100², USPS³, Yale⁴, YaleB⁵, and AR⁶, all publicly available online. Their detailed information are summarized in Table 4.1. As our goal is to rank the importance of input features, we compare our proposed method, which will name OCCA-FS, with three existing methods: T-test [17], CRFS [8], and PEB-FS [29], in terms of classification accuracy.

Table 4.1: Statistics of six datasets.

	COIL20	COIL100	USPS	Yale	AR	YaleB
number of data samples (p)	1440	7200	9298	165	840	2414
number of features (n)	1024	1024	256	1024	768	1024
number of class labels (k)	20	100	10	15	120	38

Our experiments are carried as follows. For each dataset, we first split it randomly into two subsets of 60% for training and 40% for testing, and then run each compared

¹<http://www.cs.columbia.edu/CAVE/software/softlib/coil-20.php>

²<http://www.cs.columbia.edu/CAVE/software/softlib/coil-100.php>

³<https://www.csie.ntu.edu.tw/~cjlin/libsvmtools/datasets/multiclass.html#usps>

⁴http://www.cad.zju.edu.cn/home/dengcai/Data/Yale/Yale_32x32.mat

⁵http://www.cad.zju.edu.cn/home/dengcai/Data/YaleB/YaleB_32x32.mat

⁶<http://www.cat.uab.cat/Public/Publications/1998/MaB1998/CVCRReport24.pdf>

method on the training subset to generate a ranking of the input features, finally train a one-nearest neighbor classifier on the training subset with the q top-ranked features and calculate the classification accuracy on the testing subset with the q top-ranked features. We let q vary in $[10, 20, 30, 40, 50]$ as in [29]. The same experiment is repeated ten times with different random splitting of 60% for training and 40% for testing. We report the average accuracy with standard deviation by each method in Table 4.2.

In what follows, we will compare the effectiveness of feature ranking by the four methods through classification accuracy in subsection 4.2, and then evaluate the optimization solver for solving (2.5) in PEB-FS [29] and our NEPv solver for (1.6) in OCCA-FS, respectively, in terms of empirical convergence, in subsection 4.3, and finally in subsection 4.4, we will investigate the parameter sensitivity analysis of our OCCA-FS with respect to hyper-parameter α .

4.2 Classification performance

In this subsection, we evaluate four feature selection methods: T-test [17], CRFS [8], PEB-FS [29] and our newly developed OCCA-FS, in terms of classification accuracy. For each method on a dataset, upon each random splitting into two subsets: 60% for training and 40% for testing, it first uses the training subset to generate a feature ranking for the dataset, and then a classifier on the q top-ranked features is trained, and finally, the classifier is tested on the testing subset. We report in Table 4.2 the average accuracy with standard deviation by all methods. We have the following observations:

- (i) OCCA-FS significantly outperforms the others on three datasets COIL1000, USPS and AR. OCCA-FS is competitive to T-test and CRFS on COIL20 and Yale. When a small number of the top-ranked features are used, OCCA-FS shows better performance than others. This is important because, conceivably, for the same performance, the smaller the number of selected features the more preferable.
- (ii) CRFS is competitive to OCCA-FS on two of the six datasets. CRFS works better than others on YaleB and marginally better than OCCA-FS on COIL20.
- (iii) OCCA-FS significantly outperforms PEB-FS on all six datasets for five different q , the number of selected features, except for USPS for the case of 10 selected features, despite that both methods are essentially based on the same mathematical principle because (1.6) can be viewed as the one obtained from (2.5) by optimizing scaling parameter γ out.

To the last observation, we believe, it is due to a mistake in the optimization procedure in PEB-FS [29], as we previously explained in subsection 2.2; see also subsection 4.4 below.

4.3 Empirical illustration on convergence by PEB-FS and OCCA-FS

Table 4.2 clearly shows that our OCCA-FS outperforms PEB-FS on all six datasets, and yet the two methods are essentially based on the same mathematical principle but solved differently. Previously, we pointed out a mistake in the optimization procedure in [29]

Table 4.2: Average accuracy with standard deviation over 10 random splitting of 60% for training and 40% for testing as the number q of selected features varies from 10 to 50. The best accuracies are in **bold**.

q features	dataset	T-test	CRFS	PEB-FS	OCCA-FS
10	COIL20	0.7189 \pm 0.0424	0.7128 \pm 0.0484	0.3639 \pm 0.0208	0.8521 \pm 0.0310
	COIL100	0.1752 \pm 0.0438	0.3450 \pm 0.0674	0.2255 \pm 0.0221	0.4824 \pm 0.1092
	USPS	0.6831 \pm 0.0365	0.7303 \pm 0.0198	0.7512 \pm 0.0344	0.6998 \pm 0.0587
	Yale	0.4379 \pm 0.0924	0.3879 \pm 0.0535	0.3197 \pm 0.0471	0.3970 \pm 0.0748
	AR	0.2866 \pm 0.0688	0.1899 \pm 0.0330	0.2607 \pm 0.0379	0.3482 \pm 0.0347
	YaleB	0.4366 \pm 0.0264	0.5041 \pm 0.0374	0.3879 \pm 0.0611	0.4715 \pm 0.0431
20	COIL20	0.8443 \pm 0.0480	0.9196 \pm 0.0296	0.4188 \pm 0.0308	0.9453 \pm 0.0279
	COIL100	0.3387 \pm 0.0504	0.5662 \pm 0.0711	0.3145 \pm 0.0185	0.6460 \pm 0.1038
	USPS	0.7730 \pm 0.0058	0.8732 \pm 0.0197	0.8765 \pm 0.0152	0.8828 \pm 0.0218
	Yale	0.4909 \pm 0.0806	0.4167 \pm 0.0501	0.3894 \pm 0.0452	0.4409 \pm 0.0578
	AR	0.3563 \pm 0.0588	0.2979 \pm 0.0334	0.3086 \pm 0.0217	0.4268 \pm 0.0259
	YaleB	0.5576 \pm 0.0241	0.6345 \pm 0.0251	0.5489 \pm 0.0463	0.5503 \pm 0.0439
30	COIL20	0.9012 \pm 0.0202	0.9648 \pm 0.0116	0.9521 \pm 0.0418	0.9630 \pm 0.0130
	COIL100	0.4517 \pm 0.0351	0.6885 \pm 0.0270	0.3636 \pm 0.0206	0.7768 \pm 0.0424
	USPS	0.8532 \pm 0.0031	0.9205 \pm 0.0070	0.9216 \pm 0.0075	0.9343 \pm 0.0123
	Yale	0.5000 \pm 0.1010	0.4288 \pm 0.0411	0.4273 \pm 0.0301	0.4803 \pm 0.0441
	AR	0.3836 \pm 0.0416	0.3292 \pm 0.0247	0.3461 \pm 0.0278	0.4473 \pm 0.0378
	YaleB	0.6083 \pm 0.0221	0.7086 \pm 0.0194	0.5982 \pm 0.0258	0.5968 \pm 0.0355
40	COIL20	0.9266 \pm 0.0160	0.9753 \pm 0.0100	0.9741 \pm 0.0137	0.9734 \pm 0.0064
	COIL100	0.5354 \pm 0.0288	0.7326 \pm 0.0158	0.3960 \pm 0.0109	0.8406 \pm 0.0191
	USPS	0.8926 \pm 0.0055	0.9387 \pm 0.0039	0.9398 \pm 0.0025	0.9547 \pm 0.0049
	Yale	0.5136 \pm 0.0902	0.4576 \pm 0.0478	0.4515 \pm 0.0473	0.5015 \pm 0.0454
	AR	0.4161 \pm 0.0576	0.3735 \pm 0.0253	0.3836 \pm 0.0185	0.4524 \pm 0.0450
	YaleB	0.6424 \pm 0.0216	0.7581 \pm 0.0205	0.5262 \pm 0.0282	0.6445 \pm 0.0287
50	COIL20	0.9472 \pm 0.0126	0.9807 \pm 0.0090	0.8694 \pm 0.0125	0.9793 \pm 0.0097
	COIL100	0.5849 \pm 0.0252	0.7570 \pm 0.0233	0.4053 \pm 0.0069	0.8835 \pm 0.0219
	USPS	0.9176 \pm 0.0047	0.9489 \pm 0.0026	0.9476 \pm 0.0044	0.9609 \pm 0.0032
	Yale	0.5379 \pm 0.0719	0.4455 \pm 0.0590	0.4545 \pm 0.0258	0.4955 \pm 0.0378
	AR	0.4354 \pm 0.0641	0.3884 \pm 0.0329	0.4039 \pm 0.0125	0.4628 \pm 0.0469
	YaleB	0.6500 \pm 0.0156	0.7780 \pm 0.0167	0.5428 \pm 0.0216	0.6697 \pm 0.0234

and argued that should have a lot to do with the inferior performance by PEB-FS. In this subsection, we will numerically demonstrate how objective value moves during the iterative processes by the our NEPv approach in section 3 and by the alternating solver in PEB-FS [29]. Specifically, Figure 4.1 plots one of the ten repeated runs for $\alpha = 0.01$. We observe that

- (i) OCCA-FS always ends up with a better optimizer than PEB-FS in terms of objective value for all six datasets;
- (ii) OCCA-FS enjoys monotonic convergence in objective value as guaranteed by [15, Theorems 6.3 and 6.4]; however, PEB-FS behaves erroneously for dataset Yale, contradicting [29, Theorem 3.2] which claims monotonicity in objective value by PEB-FS.

These observations show that our OCCA-FS embeds a robust optimization solver that is globally convergent, while PEB-FS [29] does not.

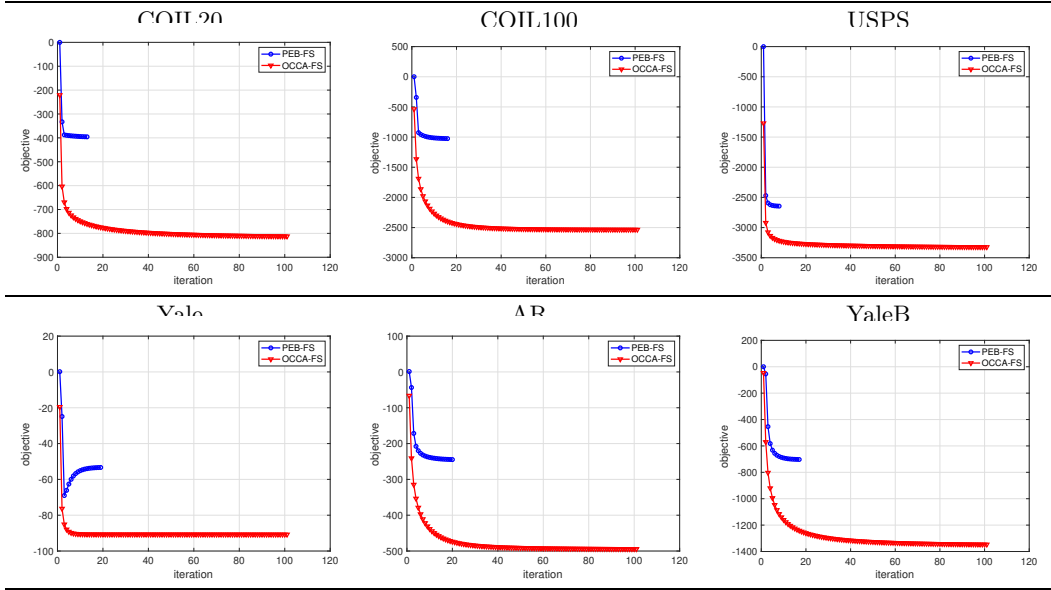


Figure 4.1: Behavior of objective values during optimization processes in OCCA-FS and PEB-FS. In terms of optimization, eventually, the smaller the objective value is, the more superior the optimization solver will be. For dataset Yale, PEB-FS does not produce monotonically decreasing objective values as claimed by [29, Theorem 3.2].

4.4 Parameter sensitivity analysis

Both mathematical models (1.6) and (2.5) contain a hyperparameter α , which is used to control the magnitudes of the 2-norm of the rows in optimizer P so as to rank input features. In order to analyze its sensitivity, we perform a sensitivity analysis based on evaluating the resulting classifiers on varying the number of selected features. Hence, besides α , the number of selected features is considered as another hyperparameter for this analysis. Specifically, we run our OCCA-FS with $\alpha \in [0.01, 0.05, 0.1, 1, 10, 100]$ and the number of selected features in $[10, 20, 30, 40, 50]$. The average accuracy by our OCCA-FS over 10 repeated experiments with respect to α and the number of selected features is shown in Figure 4.2. For a fixed number of selected features, the smaller α is, the worse the testing accuracy is on COIL20, YaleB, and COIL100, but the trend is different on USPS, AR, and Yale. For a small number of selected features, the accuracy is sensitive to α , depending on the datasets. However, when the number of selected features become large, the accuracy is less sensitive to α .

4.5 Comparisons of plain NEPv with accelerated NEPv

As the computation complexity for solving (1.6) is affected by the number of input features, we now evaluate our plain NEPv (or NEPv for short) in Algorithm 3.1 against the LOGG-accelerated NEPv (or AccNEPv for short) in Algorithm 3.2 in terms of computation time and accuracy with respect to varying the number of input features. For the task of feature selection, given a dataset, we simulate a collection of similar datasets by adding

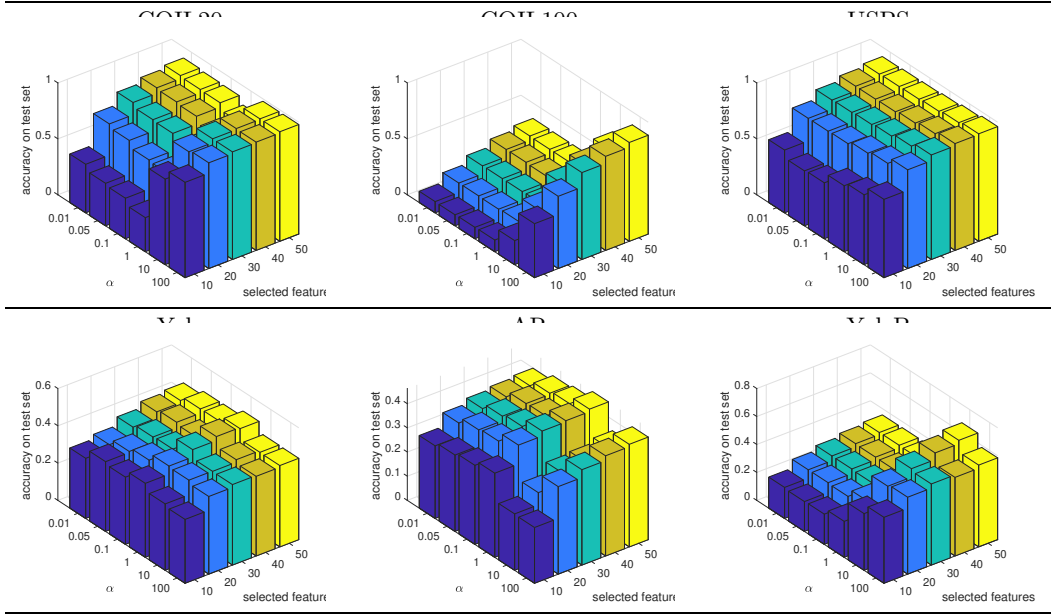


Figure 4.2: Parameter sensitivity analysis on OCCA-FS with respect to testing accuracy via varying the number q of selected features and regularization parameter α on the six datasets.

Table 4.3: CPU time (in seconds) on the simulated datasets COIL20- t

method	$t = 1$	$t = 2$	$t = 3$	$t = 4$	$t = 5$	$t = 6$
NEPv	$8.2 \cdot 10^3$	$1.7 \cdot 10^4$	$3.4 \cdot 10^4$	$6.2 \cdot 10^4$	$1.0 \cdot 10^5$	$1.5 \cdot 10^5$
AccNEPv	$4.2 \cdot 10^3$	$5.6 \cdot 10^3$	$5.7 \cdot 10^3$	$5.9 \cdot 10^3$	$5.5 \cdot 10^3$	$4.6 \cdot 10^3$

random noisy features and thereby without introducing new meaningful features. In this experiment, we take COIL20 as the base dataset, and create a pool of datasets named COIL20- t by appending $t \times 1000$ noisy features randomly drawn from the uniform distribution in the interval $(0, 0.01)$, and so the total number of input features for COIL20- t is $1024 + 1000t$. The evaluation criteria on these datasets are the same as in subsections 4.2 and 4.3, while the main focus of comparison is computational time by NEPv and AccNEPv in solving (1.6).

For comparing NEPv and AccNEPv on the six simulated datasets with input feature dimensions from 2024 to 7024 as t varies in $\{1, 2, 3, 4, 5, 6\}$, we look at how the objective value changes as a function of elapsed CPU time as the optimization process proceeds. This is plotted in Figure 4.3. First, AccNEPv not only achieves the objective value similar to NEPv, but also run much faster than NEPv. Second, from Table 4.3 as the number of input features increases, the speed-up of AccNEPv over NEPv increases too. Third, AccNEPv performs competitively to NEPv in terms of classification accuracy.

These experiments on the simulated datasets COIL20- t reveal that the plain NEPv can be impractical for datasets with more than 10^4 features. Unfortunately, that kind of sizes is quite common when it comes to text classification, for which the number of

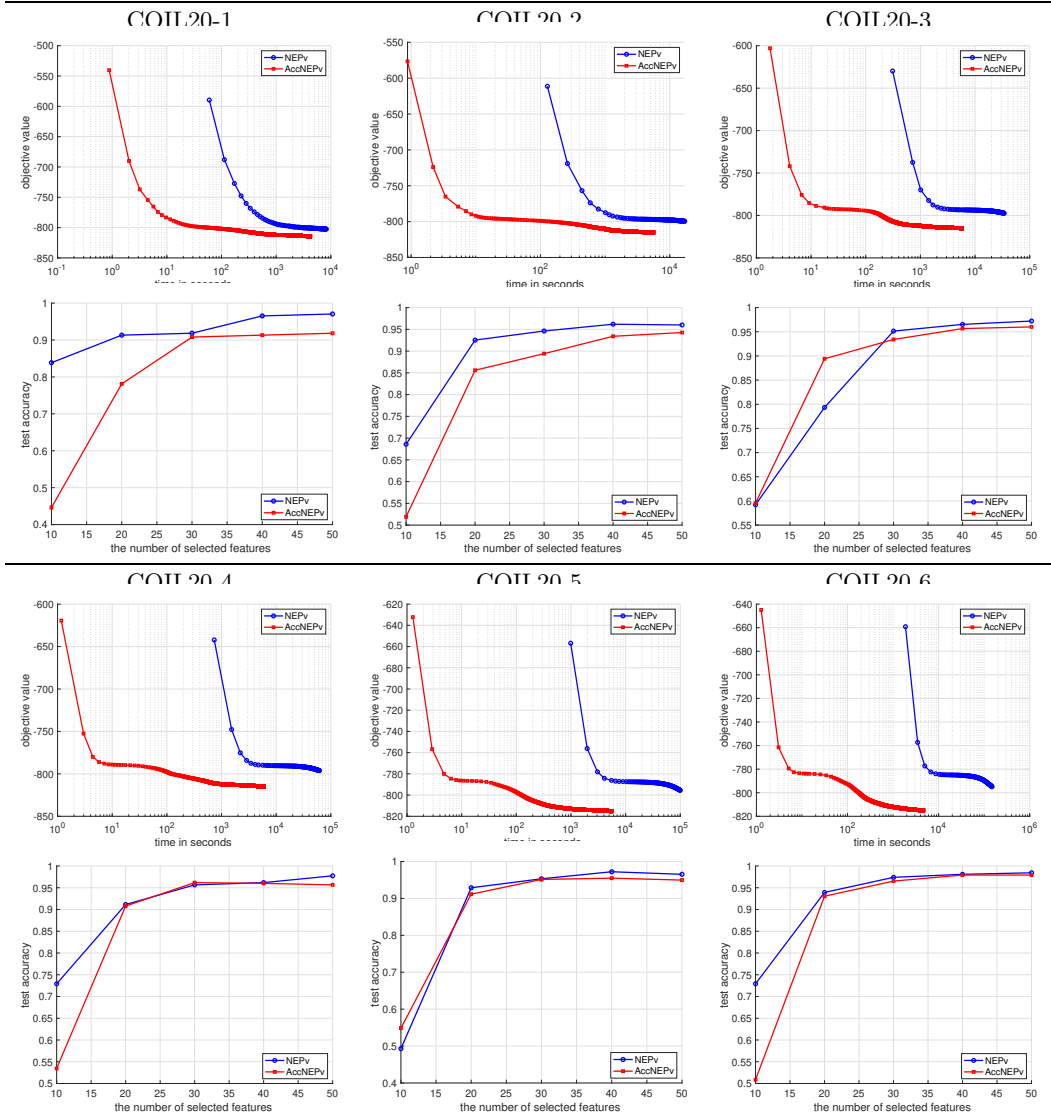


Figure 4.3: Comparison between NEPv and AccNEPv in terms of objective value during the NEPv optimization processes and classification accuracy on datasets COIL20- t for $t \in \{1, 2, 3, 4, 5, 6\}$.

features is the number of words and often there are more than 10^4 words, as it can be seen from Table 4.4, where the statistics of four publicly available text datasets⁷ is displayed. In what follows, we report our experimental results on these four datasets by AccNEPv only because the numbers of words in the datasets are too large for NEPv to finish its computations within reasonable amount of time (like in a day). Figure 4.4 and Table 4.5 summarize our experimental results by AccNEPv. From Figure 4.4, it can be seen that AccNEPv converges very fast and yields good classification accuracy. AccNEPv takes

⁷<http://www.cad.zju.edu.cn/home/dengcai/Data/TextData.html>

Table 4.4: Statistics of the four text datasets.

	RCV1_4Class	Reuters21578	TDT2	20NewsHome
number of documents (p)	9625	8293	9394	18774
number of words (n)	29992	18933	36771	61188
number of class labels (k)	4	65	30	20

a few hours to finish the experiments as indicated by Table 4.5. For example, NEPv takes about 12 hours for 20NewsHome, which has more than 60 thousands of features and 18 thousands of documents. These experimental results demonstrate that AccNEPv is effective and works very well for large-scale high-dimensional real-world datasets.

Table 4.5: CPU time (in hours) by AccNEPv on the four text datasets.

dataset	RCV1_4Class	Reuters21578	TDT2	20NewsHome
AccNEPv	9.98	10.97	11.19	12.46

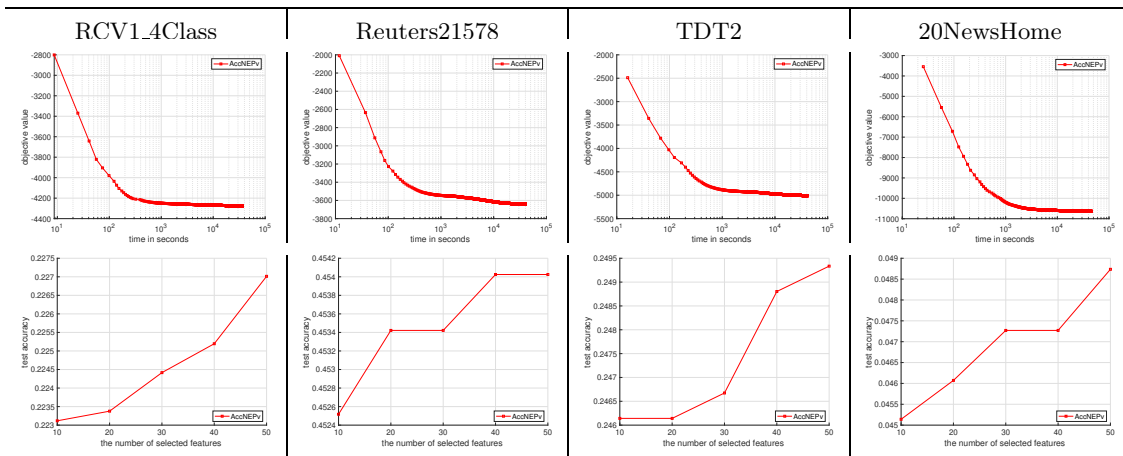


Figure 4.4: Experimental results by AccNEPv on the four text datasets in Table 4.4 in terms of both objective value during optimization iterations and classification accuracy.

5 Conclusion

In this paper, motivated by orthogonal canonical correlation analysis (OCCA) [28], we propose a novel supervised feature selection model that combines OCCA with the $(2, 1)$ -norm regularization, which we call OCCA21. It is explained that the new model has a close mathematical connection to the supervised feature selection model OLSR-OS21 (orthogonal least squares regression with optimal scaling and with the $(2, 1)$ -norm regularization) [29]. It turns out that OCCA21 falls into the class of optimization problems

on the Stiefel manifold, because of (3.1), for which the NEPv approach [15] is theoretically sound and numerically efficient. Through numerical experiments, we demonstrate the performances of our eventual feature selection method, OCCA-FS, in comparison with PEB-FS and other state-of-the-art feature selection methods in the literature, in the areas of both numerical optimization and feature selection. It is concluded that OCCA-FS computes much better optimizers than PEB-FS, produces superior classification performance to PEB-FS and often OCCA-FS comes out on the top among all feature selection methods in comparison.

It is noted that in [29] OLSR-OS21 is solved alternatingly between its two optimizing variables. Unfortunately, one of the two alternating updates is not done correctly, invalidating the major convergence claim in [29]. That incorrectness inevitably affects the classification performance of PEB-FS, the eventual feature selection method of [29], as confirmed by our extensive numerical experiments.

References

- [1] P. Benner and X. Liang. Convergence analysis of vector extended locally optimal block preconditioned extended conjugate gradient method for computing extreme eigenvalues. *Numer. Linear Algebra Appl.*, 29(6):e2445, 2022. 24 pages.
- [2] S. Boyd and L. Vandenberghe. *Convex Optimization*. Cambridge University Press, Cambridge, UK, 2004.
- [3] D. Cai, X. He, J. Han, and H.-J. Zhang. Orthogonal laplacian faces for face recognition. *IEEE Trans. Imag. Processing*, 15(11):3608–3614, 2006.
- [4] J. Demmel. *Applied Numerical Linear Algebra*. SIAM, Philadelphia, PA, 1997.
- [5] L. Eldén and H. Park. A procrustes problem on the Stiefel manifold. *Numer. Math.*, 82:599–619, 1999.
- [6] I. Guyon and A. Elisseeff. An introduction to variable and feature selection. *J. Mach. Learning Res.*, 3(Mar):1157–1182, 2003.
- [7] I. Guyon, J. Weston, S. Barnhill, and V. Vapnik. Gene selection for cancer classification using support vector machines. *Machine Learning*, 46:389–422, 2002.
- [8] R. He, T. Tan, L. Wang, and W.-S. Zheng. l_2, l_1 regularized correntropy for robust feature selection. In *2012 IEEE Conference on Computer Vision and Pattern Recognition*, pages 2504–2511. IEEE, 2012.
- [9] N. J. Higham. *Functions of Matrices: Theory and Computation*. Society for Industrial and Applied Mathematics, Philadelphia, PA, USA, 2008.
- [10] A. Imakura, R.-C. Li, and S.-L. Zhang. Locally optimal and heavy ball GMRES methods. *Japan J. Indust. Appl. Math.*, 33:471–499, 2016.
- [11] A. V. Knyazev. Toward the optimal preconditioned eigensolver: Locally optimal block preconditioned conjugate gradient method. *SIAM J. Sci. Comput.*, 23(2):517–541, 2001.
- [12] R.-C. Li. A perturbation bound for the generalized polar decomposition. *BIT*, 33:304–308, 1993.

- [13] R.-C. Li. Matrix perturbation theory. In L. Hogben, R. Brualdi, and G. W. Stewart, editors, *Handbook of Linear Algebra*, Chapter 21. CRC Press, Boca Raton, FL, 2nd edition, 2014.
- [14] R.-C. Li. Rayleigh quotient based optimization methods for eigenvalue problems. In Z. Bai, W. Gao, and Y. Su, editors, *Matrix Functions and Matrix Equations*, volume 19 of *Series in Contemporary Applied Mathematics*, pages 76–108. World Scientific, Singapore, 2015.
- [15] R.-C. Li. A theory of the NEPv approach for optimization on the Stiefel manifold. *Found. Comput. Math.*, 2024. 64 pages, to appear.
- [16] D. Lu and R.-C. Li. Locally unitarily invariantizable NEPv and convergence analysis of SCF. *Math. Comp.*, 93(349):2291–2329, 2024.
- [17] D. C. Montgomery, G. C. Runger, and N. F. Hubele. *Engineering Statistics*. John Wiley & Sons, 2009.
- [18] B. N. Parlett. *The Symmetric Eigenvalue Problem*. SIAM, Philadelphia, 1998. This SIAM edition is an unabridged, corrected reproduction of the work first published by Prentice-Hall, Inc., Englewood Cliffs, New Jersey, 1980.
- [19] B. T. Polyak. *Introduction to Optimization*. Optimization Software, New York, 1987.
- [20] Y. Saad. *Numerical Methods for Large Eigenvalue Problems*. Manchester University Press, Manchester, UK, 1992.
- [21] Y. Saeys, I. Inza, and P. Larranaga. A review of feature selection techniques in bioinformatics. *Bioinformatics*, 23(19):2507–2517, 2007.
- [22] I. Takahashi. A note on the conjugate gradient method. *Inform. Process. Japan*, 5:45–49, 1965.
- [23] L. Wang, L.-H. Zhang, and R.-C. Li. Maximizing sum of coupled traces with applications. *Numer. Math.*, 152:587–629, 2022.
- [24] L. Wang, L.-H. Zhang, and R.-C. Li. Trace ratio optimization with an application to multi-view learning. *Math. Program.*, 201:97–131, 2023.
- [25] X. Wu, X. Xu, J. Liu, H. Wang, B. Hu, and F. Nie. Supervised feature selection with orthogonal regression and feature weighting. *IEEE Trans. Neural Net. Learn. Sys.*, 32(5):1831–1838, 2020.
- [26] M. Yang and R.-C. Li. Heavy ball flexible GMRES method for nonsymmetric linear systems. *J. Comp. Math.*, 40(5):715–731, 2021.
- [27] L.-H. Zhang, W. H. Yang, C. Shen, and J. Ying. An eigenvalue-based method for the unbalanced Procrustes problem. *SIAM J. Matrix Anal. Appl.*, 41(3):957–983, 2020.
- [28] L.-H. Zhang, L. Wang, Z. Bai, and R.-C. Li. A self-consistent-field iteration for orthogonal canonical correlation analysis. *IEEE Trans. Pattern Anal. Mach. Intell.*, 44(2):890–904, 2022.
- [29] R. Zhang, F. Nie, and X. Li. Feature selection under regularized orthogonal least square regression with optimal scaling. *Neurocomputing*, 273:547–553, 2018.